



# EDGEWOOD CHEMICAL BIOLOGICAL CENTER

U.S. ARMY RESEARCH, DEVELOPMENT AND ENGINEERING COMMAND  
Aberdeen Proving Ground, MD 21010-5424

ECBC-TR-1528

## TRANSLATIONAL HUMAN HEALTH ASSESSMENT OF CARFENTANIL USING AN EXPERIMENTALLY REFINED PBPK MODEL

Michael G. Feasel  
Richard J. Lawrence  
Robert L. Kristovich

RESEARCH AND TECHNOLOGY DIRECTORATE

Ariane Wohlfarth  
Marilyn A. Huestis

NATIONAL INSTITUTE ON DRUG ABUSE  
Baltimore, MD 21224-2816

September 2018

Approved for public release: distribution unlimited.



### Disclaimer

The findings in this report are not to be construed as an official Department of the Army position unless so designated by other authorizing documents.

# REPORT DOCUMENTATION PAGE

Form Approved  
OMB No. 0704-0188

Public reporting burden for this collection of information is estimated to average 1 h per response, including the time for reviewing instructions, searching existing data sources, gathering and maintaining the data needed, and completing and reviewing this collection of information. Send comments regarding this burden estimate or any other aspect of this collection of information, including suggestions for reducing this burden to Department of Defense, Washington Headquarters Services, Directorate for Information Operations and Reports (0704-0188), 1215 Jefferson Davis Highway, Suite 1204, Arlington, VA 22202-4302. Respondents should be aware that notwithstanding any other provision of law, no person shall be subject to any penalty for failing to comply with a collection of information if it does not display a currently valid OMB control number. **PLEASE DO NOT RETURN YOUR FORM TO THE ABOVE ADDRESS.**

<b>1. REPORT DATE (DD-MM-YYYY)</b> XX-09-2018		<b>2. REPORT TYPE</b> Final		<b>3. DATES COVERED (From - To)</b> Dec 2015–Apr 2017	
<b>4. TITLE AND SUBTITLE</b> Translational Human Health Assessment of Carfentanil Using an Experimentally Refined PBPK Model				<b>5a. CONTRACT NUMBER</b>	
				<b>5b. GRANT NUMBER</b>	
				<b>5c. PROGRAM ELEMENT NUMBER</b>	
<b>6. AUTHOR(S)</b> Feasel, Michael G.; Lawrence, Richard J.; Kristovich, Robert L. (ECBC); Wohlfarth, Ariane; Huestis, Marilyn A. (NIDA)				<b>5d. PROJECT NUMBER</b> CB3281	
				<b>5e. TASK NUMBER</b>	
				<b>5f. WORK UNIT NUMBER</b>	
<b>7. PERFORMING ORGANIZATION NAME(S) AND ADDRESS(ES)</b> Director, ECBC, ATTN: RDCB-DRT-O, APG, MD 21010-5424 National Institute on Drug Abuse, National Institutes of Health; 251 Bayview Boulevard, Baltimore, MD 21224-2816				<b>8. PERFORMING ORGANIZATION REPORT NUMBER</b> ECBC-TR-1528	
<b>9. SPONSORING / MONITORING AGENCY NAME(S) AND ADDRESS(ES)</b> Defense Threat Reduction Agency, 8725 John J. Kingman Road, MSC 6201, Fort Belvoir, VA 22060-6201				<b>10. SPONSOR/MONITOR'S ACRONYM(S)</b> DTRA	
				<b>11. SPONSOR/MONITOR'S REPORT NUMBER(S)</b>	
<b>12. DISTRIBUTION / AVAILABILITY STATEMENT</b> Approved for public release: distribution unlimited.					
<b>13. SUPPLEMENTARY NOTES</b>					
<b>14. ABSTRACT:</b> Methods for measuring acute toxicity and risk assessments for acutely toxic materials require large numbers of animal subjects, multiple species, specialized infrastructure, and personnel training. This study demonstrated that carfentanil toxicity can be accurately modeled using a physiologically based pharmacokinetic (PBPK) model refined with in vitro and ex vivo experimental data and a limited in vivo animal study. Experiments were performed to measure plasma protein binding, blood partitioning, and microsomal clearance in rabbit and human plasma, whole blood, and liver microsomes, respectively. Rabbit properties were incorporated into a rabbit physiology within the PBPK model, and kinetics were compared with those of a small cohort of rabbits exposed intravenously to carfentanil. The properties refined the predicted kinetics to reflect those seen in vivo as a validation of the PBPK model. Upon successful validation in the rabbit physiology, the model was changed to human physiology, populated with human data, and optimized for dose-equivalence. The equivalent human dose to a loss of righting reflex endpoint as indicated by the rabbit surrogate was 0.34 µg/kg. This confirms that carfentanil is an acutely toxic material and provides, for the first time, a human toxic dose without a need for forensic toxicology or non-physiological extrapolation.					
<b>15. SUBJECT TERMS</b>					
Opioid		Risk assessment			
Carfentanil		Clearance			
Physicochemical		Modeling			
Physiologically based pharmacokinetic (PBPK)		Human estimate			
<b>16. SECURITY CLASSIFICATION OF:</b>			<b>17. LIMITATION OF ABSTRACT</b>	<b>18. NUMBER OF PAGES</b>	<b>19a. NAME OF RESPONSIBLE PERSON</b>
<b>a. REPORT</b>	<b>b. ABSTRACT</b>	<b>c. THIS PAGE</b>			<b>19b. TELEPHONE NUMBER (include area code)</b>
U	U	U	UU	34	Renu B. Rastogi (410) 436-7545

Standard Form 298 (Rev. 8-98)  
Prescribed by ANSI Std. Z39.18

Blank

## **PREFACE**

The work described in this report was authorized under project no. CB3281. The work was started in December 2015 and completed in April 2017.

The use of either trade or manufacturers' names in this report does not constitute an official endorsement of any commercial products. This report may not be cited for purposes of advertisement.

This report has been approved for public release.

Blank

# CONTENTS

	PREFACE.....	iii
1.	INTRODUCTION .....	1
2.	MATERIALS AND METHODS.....	3
2.1	Chemicals and Reagents .....	3
2.2	RLM Stability Study .....	4
2.2.1	Incubations .....	4
2.2.2	Sample Preparation .....	4
2.2.3	Instrumentation .....	4
2.2.4	LC–MS Analysis.....	5
2.3	Physicochemical Properties .....	5
2.3.1	Incubations: Plasma Protein Binding.....	5
2.3.2	Incubations: Blood Partitioning by Depletion .....	6
2.3.3	Sample Preparation for Analysis .....	6
2.3.4	LC–MS/MS Analysis.....	6
2.4	In Vivo Exposure of Rabbits to Carfentanil .....	7
2.5	Human and Rabbit PBPK Profile Simulations Using GastroPlus Software.....	8
3.	RESULTS .....	8
3.1	Carfentanil Stability Study in RLMs .....	8
3.2	Physicochemical Properties for HLMs and Hepatocytes.....	9
3.3	In Silico Predictions of Physicochemical Properties .....	9
3.4	In Vivo PK Study of Carfentanil in Rabbits .....	10
3.5	In Silico Modeling of Rabbit PK .....	11
3.6	In Silico Prediction of Bioequivalent Dose of Carfentanil .....	15
4.	DISCUSSION AND CONCLUSIONS .....	16
	LITERATURE CITED.....	19
	ACRONYMS AND ABBREVIATIONS .....	23

## FIGURES

1.	Stepwise schematic for predicting PK with various levels of experimental data.....	3
2.	Parent compound depletion of carfentanil in RLM incubation .....	9
3.	PK data for NZWRs dosed at 1.0 µg/kg of carfentanil.....	11
4.	Naïve PBPK model obtained using only predicted ADMET Predictor properties, based on the two-dimensional structure of carfentanil .....	12
5.	PBPK model incorporating only $CL_{int}$ .....	13
6.	PBPK prediction incorporating only plasma protein binding experimental data .....	13
7.	PBPK model incorporating only RBC plasma partitioning (RBP).....	14
8.	PBPK model incorporating $CL_{int}$ , RBP, and plasma protein binding .....	15
9.	Human-equivalent dosing of carfentanil extrapolated from in silico model of rabbit PK data .....	16

## TABLES

1.	Preparation Volumes for Matrix-Matched RED Samples .....	5
2.	Physicochemical Properties of Carfentanil with Benchmark Compound Fentanyl and Carfentanil Metabolite Norcarfentanil .....	10
3.	Therapeutic Toxic Doses for Carfentanil in Monkeys (Port et al.) and Humans (Newberg et al.) and Their Respective Therapeutic Indices .....	17



# TRANSLATIONAL HUMAN HEALTH ASSESSMENT OF CARFENTANIL USING AN EXPERIMENTALLY REFINED PBPK MODEL

## 1. INTRODUCTION

The performance of human risk assessments for acutely toxic materials (e.g., chemical warfare agents) requires specialized infrastructure, test facilities, and trained personnel. Dosing multiple species by different exposure routes takes time; however, military and/or civilian regulatory agencies have a critical need for toxicological data. If an acute exposure occurs, human risk assessments are not exclusively employed clinically; rather, they are used to guide personal and collective protection, detector development, and decontamination requirements, with the goal of protecting end-users from contamination. For this reason, demands for high-confidence human risk assessments are outpacing traditional methods of acute toxicological assessment.

In this work, a human risk assessment for the ultra-potent opioid carfentanil was generated using *in silico* physiologically based pharmacokinetic (PBPK) modeling software. The software was refined with *in vitro* experimental data to replace some key physicochemical and physiological properties that most greatly influence pharmacokinetics and toxicokinetics. The kinetic model was then validated using a small cohort of a surrogate species (rabbits). The PBPK software was used to translate the rabbit model results to a human-equivalent dose.

Carfentanil was used in the resolution of a 2002 hostage situation in Moscow, Russia and appeared on the illicit drug market in 2016 (1–5). The novelty of this research is the carfentanil clinical data pertaining to humans. The only human risk assessment or estimate of a toxic dose was provided by the U.S. Drug Enforcement Administration (DEA; Washington, DC). This estimate was based on carfentanil's therapeutic potency, as compared with its better-studied congener, fentanyl, which has ~1/100th the potency of carfentanil (6). It is problematic when the surrogate species selected (in this case, the rodent model) is a poor model of toxicity despite its utility in measuring therapeutic endpoints.

The animal model selected is vital to the successful translation of xenobiotic effects to humans. Having an appropriate animal model for the drug's mechanism of action and its potential off-target or adverse-outcome pathways is ideal. Fentanyl was first screened in mice and rats, which are animals with a wide therapeutic index or difference between therapeutic and lethal doses. Mice and rats provide good therapeutic models for measuring nociception (7); however, their toxic and lethal responses are not representative of those for higher-order species. Humans are more susceptible to toxic opioid effects and have an order of magnitude lower therapeutic index.

The surrogate species chosen for modeling carfentanil effects was the New Zealand White rabbit (NZWR; *Oryctolagus cuniculus*). Rabbits are good models for examining opioid therapy and opioid-induced respiratory depression at lower doses than are used in rodents (i.e., rabbits have a smaller therapeutic index) (8–10).

To better model any species' *in vivo* pharmacokinetics (PK) data and translate the *in silico* modeling from rabbit to human, experimentally derived values for drug clearance (obtained using species-appropriate liver microsomes) and experimentally derived physicochemical properties (calculated using species-appropriate blood fractions) populated the model. Drug clearance is the single most important modeling parameter (11). Clearance, while influenced by the appropriate prediction or experimental determination of physicochemical properties, affects predicted exposure in the central compartment, circulation, and thus affects bioavailability over time. Therefore, when building a model to predict human PK, it is crucial that clearance be scaled properly for human prediction, or known in the case of modeling surrogate animal kinetics. Human intrinsic clearance was recently calculated for carfentanil (12), and the same study was performed in rabbit liver microsomes (RLMs) to calculate intrinsic clearance in the rabbit surrogate. Rabbit microsomal half-life was used to derive intrinsic clearance values, which were incorporated in the rabbit physiology of the PBPK model.

Other influences on pharmacological properties include the compound's physicochemical properties, none of which were experimentally derived for carfentanil. This study aimed to establish, in human-based *in vitro* assays, the plasma protein binding and blood partitioning of carfentanil. Plasma protein binding influences how quickly a drug is cleared from the systemic circulation, and how much of the drug is available to act on its receptor targets. Blood partitioning indicates whether the red blood cells (RBCs) act as a reservoir for the compound. Results of blood partitioning indicate which biosample is best suited to detect minute quantities of drug that can elicit a therapeutic or toxic response in humans (13).

Physicochemical properties such as plasma protein binding and blood partitioning are key modeling parameters because they directly influence how much unbound drug is free in the systemic circulation and where the free drug goes within the central blood compartment (11). Because carfentanil exhibits high lipophilicity, it is a candidate for sequestration in lipid bilayers and membranes, including those of the RBCs (14, 15). If carfentanil migrates heavily into the RBCs, they can act as a sink, thereby prolonging exposure (16). Knowledge of blood partitioning will guide forensic specialists and medical personnel toward the proper sampling protocol, namely, whole blood, plasma, or serum (17, 18).

We used GastroPlus v.9.0.0007 *in silico* PBPK model software (Simulations Plus; Lancaster, CA), which is preferred over traditional compartmental models because each organ system (and all of its physiological properties) is treated as its own compartment. Properties include perfusion rates, partitioning coefficients, and cytochrome P450 enzyme contents and activities (19) for a specific organ or tissue and a specific species. PBPK models are also more useful when attempting to translate among species. GastroPlus software is built on the PK properties of human physiologies for various ethnicities, and it can scale according to age, weight, gender, and model species. The software models physiologies for the gut, liver, lung, spleen, heart, brain, kidney, skin, adipose tissue, venous and arterial blood, and yellow and red marrows.

First, we compared a naïve rabbit PBPK model (i.e., purely predicted properties based solely on chemical structure) to the PK that were observed *in vivo* after intravenous (iv) exposures of rabbits to single carfentanil doses. Experimentally derived data were substituted for the predicted intrinsic clearance and physicochemical properties in a stepwise fashion, and the

model was run between each data point replacement. This enabled assessment of the properties that influenced the model to be more representative of in vivo exposures. Finally, equivalent dosing in humans was determined by switching to human physiology, substituting experimental human liver microsome (HLM) intrinsic clearance and each of the human-based physicochemical properties, and optimizing for the administered dose (Figure 1).

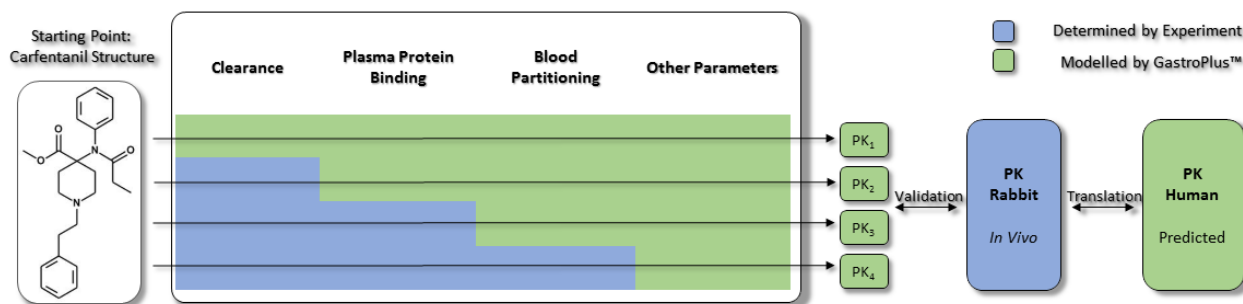


Figure 1. Stepwise schematic for predicting PK with various levels of experimental data. PK<sub>1</sub> represents kinetics derived entirely from prediction based on the chemical structure. PK<sub>2</sub> represents a kinetic model incorporating in vitro clearance data.

## 2. MATERIALS AND METHODS

### 2.1 Chemicals and Reagents

*Caution: Carfentanil is hazardous and should be handled carefully: multiple Narcan (naloxone hydrochloride; Adapt Pharma; Radnor, PA) intranasal or intramuscular devices per person should be readily available, and a buddy system should be employed. Butyl rubber gloves are highly recommended when handling carfentanil materials or solutions.*

Carfentanil citrate (95.8% pure, as determined by <sup>1</sup>H and <sup>13</sup>C NMR) was synthesized at the U.S. Army Edgewood Chemical Biological Center (ECBC; Aberdeen Proving Ground, MD). A 1.0 mg/mL solution, adjusted for citrate salt formulation and purity, was prepared gravimetrically in liquid chromatography–mass spectrometry (LC–MS) grade methanol purchased from Sigma-Aldrich (St. Louis, MO). LC–MS grade water and formic acid were acquired from Fisher Scientific (Fair Lawn, NJ), and LC–MS grade acetonitrile (ACN) was obtained from Sigma-Aldrich. Isopropanol (American Chemical Society reagent grade, 99.6%) was obtained from Acros Organics (VWR; West Chester, PA). Reduced nicotinamide adenine dinucleotide phosphate (NADPH)-regenerating system solutions A (part no. 451220) and B (part no. 451200) were purchased from Corning (Corning, NY). Norcarfentanil was acquired from Toronto Research Chemicals (Toronto, ONT) and fentanyl was from Mallinckrodt Pharmaceuticals (St. Louis, MO). Solutions for protein binding and RBC partitioning experiments were prepared at 10 mM (free base) in European Pharmacopoeia- and U.S. Pharmacopoeia-grade dimethyl sulfoxide (DMSO) (Sigma-Aldrich). Isotopically labeled internal standard (ISTD) compounds were obtained from Toronto Research Chemicals and were prepared at 4.9 mg/mL (carfentanil-*d*<sub>5</sub>, free base) and 1.0 mg/mL (norcarfentanil-*d*<sub>5</sub>, free base) in

methanol. Fentanyl-*d*<sub>5</sub> was purchased from Cerilliant Corporation (Round Rock, TX) as a methanolic solution (100 µg/mL, free base). All solutions were stored at –20 °C until use.

Phosphate-buffered saline (PBS; 10×) was obtained from Electron Microscopy Sciences (Hatfield, PA) and diluted 1:10 with deionized water (dH<sub>2</sub>O) from a Millipore (Darmstadt, Germany) water purification system. The resultant salt concentrations were 2.7 mM potassium chloride, 10 mM disodium phosphate, and 137 mM sodium chloride. The pH was verified as 7.4, and the solution was stored at 4 °C until use.

Male and female human and rabbit heparinized whole blood and plasma were obtained from BioIVT (Westbury, NY) and stored at 4 and –80 °C, respectively, until required.

## **2.2 RLM Stability Study**

### **2.2.1 Incubations**

This experiment was performed in accordance with our previous studies of HLMs (12).

For the rabbit liver RLM incubations, carfentanil (5 µmol/L) was incubated for 1 h at 37 °C, under constant shaking, with 1 mL of a solution containing RLMs (1 mg of protein/mL; BioIVT). RLM suspensions were prepared in duplicate by adding 100 µL of 100 mmol/L potassium phosphate buffer at pH 7.4, 100 µL of 100 µg/mL carfentanil solution, 50 µL of NADPH-regenerating solution A, 10 µL of NADPH-regenerating solution B, and 50 µL of RLMs (20 mg/mL) to 690 µL of purified water. Samples (100 µL) were collected at 0, 3, 8, 13, 20, 30, 45, and 60 min and were immediately mixed with an equal volume of ice-cold ACN. Samples were stored at –80 °C before analysis.

### **2.2.2 Sample Preparation**

RLM samples were centrifuged at 4 °C for 5 min at 15,000g to remove debris. Supernatants were diluted 1:5 with mobile phase A (0.1% formic acid in water), and 10 µL was injected into the MS system. Mobile phase A, mobile phase B (0.1% formic acid in ACN, 90:10, v/v), and a neat standard of carfentanil (10 µg/L) in mobile phases A and B were also analyzed.

### **2.2.3 Instrumentation**

RLM samples were analyzed on a 3200 Qtrap mass spectrometer (Sciex; Redwood City, CA) and data were acquired with Analyst v1.6 software (Sciex). Chromatographic separation was performed on a Prominence high-performance liquid chromatography system (Shimadzu Scientific Instruments; Columbia, MD) that consisted of two LC-20 AD XR pumps, a DGU-20A5R degasser, an SIL-20 AC XR autosampler, and a CTO-20 AC column oven.

## 2.2.4 LC–MS Analysis

Chromatographic separations were performed on a Kinetex C18 column (100 × 2.1 mm, 2.6 μm; Phenomenex; Torrance, CA). Gradient elution was as follows: 10% mobile phase B from 0 to 0.5 min, ramping up to 95% mobile phase B from 0.5 to 10 min, holding 95% mobile phase B from 10 to 12.5 min, followed by re-equilibration of 10% mobile phase B at 12.5 min until completion at 15 min. LC flow was 0.5 mL/min. MS parameters were as follows: interface, positive electrospray ionization (ESI) mode; gas 1 and 2, nitrogen, at 50 psi; curtain gas, nitrogen, at 40 psi; source temperature, 500 °C; and ion spray voltage, 5500 V. The transitions monitored were charge-to-mass ratio ( $m/z$ ) 395.2/335.3 (collision energy [CE], 25 eV),  $m/z$  395.2/113.1 (CE, 39 eV), and  $m/z$  395.2/246.2 (CE, 27 eV), in agreement with published carfentanil transitions (20). Declustering potential (DP), entrance potential (EP), and collision cell exit potential (CXP) were optimized to the following values: DP, 51 V; EP, 4.5 V; and CXP, 4 V.

## 2.3 Physicochemical Properties

### 2.3.1 Incubations: Plasma Protein Binding

Single-use, rapid equilibrium dialysis (RED) 96-well plates with an 8 kDa molecular weight cutoff (Thermo Scientific; Waltham, MA) were used to measure plasma protein binding properties for carfentanil and norcarfentanil. Human and rabbit plasma were thawed and centrifuged (2300g for 15 min) to remove particulates, and 1.0 and 10 μM test concentrations were prepared in human and rabbit plasma (0.01 and 0.1% DMSO, v/v). For each test concentration, nine aliquots of 300 μL of test plasma with 500 μL of PBS buffer were added to adjoining wells of an RED plate, thereby allowing for three experiments for each concentration and time point. Unadulterated plasma experiments were included for analytical quality control blanks. Each plate was covered with adhesive sealing tape and incubated at 37 °C with platform mixing. Aliquots were transferred to micro-centrifuge tubes at 2 h intervals (2, 4, and 6 h). Aliquots were matrix-matched before LC–MS/MS sample preparation and analysis were performed, as indicated in Table 1.

Table 1. Preparation Volumes for Matrix-Matched RED Samples

<b>Hu Test Concentration</b>	<b>Transfer Volume (μL)</b>	<b>Matrix Match</b>	<b>Additional</b>
1 μM RED plasma	100	100 μL of PBS	
1 μM RED PBS	100	100 μL of Hu plasma	90 μL of
10 μM RED plasma	10	100 μL of PBS	Hu plasma
10 μM RED PBS	100	100 μL of Hu plasma	
<b>Rb Test Concentration</b>	<b>Transfer Volume (μL)</b>	<b>Matrix Match</b>	<b>Additional</b>
1 μM RED plasma	100	100 μL of PBS	
1 μM RED PBS	100	100 μL of Rb plasma	90 μL of
10 μM RED plasma	10	100 μL of PBS	Rb plasma
10 μM RED PBS	100	100 μL of Rb plasma	

Hu, human; Rb, rabbit.

### **2.3.2 Incubations: Blood Partitioning by Depletion**

Aliquots of whole blood were centrifuged (1200 g for 10 min) to generate common-origin plasma for fortifying and reference solutions. Fortifying solutions of 10  $\mu\text{M}$  fentanyl, carfentanil, and norcarfentanil were prepared in plasma from 10 mM DMSO stock. RBC partitioning experiments were conducted at 30 and 500 nM concentrations. Each 30 nM whole blood test solution was prepared by adding 15  $\mu\text{L}$  of the 10  $\mu\text{M}$  fentanyl, carfentanil, or norcarfentanil fortifying solution to 4985  $\mu\text{L}$  of whole blood. Each 500 nM whole blood test solution was prepared similarly (250 to 4750  $\mu\text{L}$ ). The blood test solutions were gently mixed with inversion. Reference plasma solutions (30 and 500 nM) were also prepared by substituting common-origin plasma for whole blood.

Each whole blood test and reference plasma solution was evenly distributed into five micro-centrifuge tubes. The tubes were labeled for 0, 10, 30, 60, and 120 min time points. The 10–120 min tubes were incubated at 37 °C with rotational mixing. At each time point, whole blood test and reference plasma tubes were removed from incubation. The whole blood test solution tubes were centrifuged, and the resulting plasma was transferred to clean micro-centrifuge tubes and mixed. Three 100  $\mu\text{L}$  aliquots were transferred to clean micro-centrifuge tubes to examine preparation and analysis in triplicate. The reference plasma tubes were vortex-mixed and aliquoted.

For each lot of whole blood, the hematocrit was measured using a HemaTrue veterinary hematology analyzer (Heska Corporation; Loveland, CO).

### **2.3.3 Sample Preparation for Analysis**

Plasma samples were fortified with ISTD and mixed. Proteins were precipitated with ACN containing 0.1% formic acid (v/v). Samples were mixed, batched, and stored overnight at –80 °C.

For analysis, samples were thawed, mixed, and centrifuged. For filtration and removal of phospholipids, the supernatants were transferred to a HybridSPE-Phospholipid 96-well protein precipitation plate (Sigma-Aldrich) that had been pretreated with ACN and 0.1% formic acid (v/v). A vacuum was applied to transfer the samples into a 96-well collection plate. The collection plate was dried using a TurboVap 96 automated evaporation system (Biotage; Charlotte, NC). The samples were reconstituted with 100  $\mu\text{L}$  of 90:10 dH<sub>2</sub>O–ACN, covered with a cap mat, mixed for 5 min, and transferred to the autosampler for LC–MS/MS analysis.

### **2.3.4 LC–MS/MS Analysis**

The analytical instrumentation for quantitative carfentanil and norcarfentanil analyses consisted of a 6490 triple-quadrupole LC–MS/MS system equipped with a 1290 Infinity LC stack that had a binary pump, an autosampler, and a column heater (Agilent Technologies; Santa Clara, CA). Agilent MassHunter workstation software was used for data acquisition and analysis. Reverse-phase separation was conducted with a Waters Corporation (Milford, MA) Acquity UPLC ethylene-bridged hybrid (BEH) 1.7  $\mu\text{m}$ , 2.1  $\times$  50 mm column, with a phase-matched VanGuard guard column that was isothermal at 40 °C. Mobile phase A consisted of

dH<sub>2</sub>O with 0.1% formic acid, and mobile phase B was ACN with 0.1% formic acid. For carfentanil, a 2 min gradient elution starting with 10% mobile phase B for 0.5 min, to 99% mobile phase B at 1 min, hold for 0.5 min, and return to initial conditions and equilibrate for 0.5 min. For norcarfentanil, a 3 min gradient elution starting with 15% mobile phase B for 1 min, to 99% mobile phase B at 1.5 min, hold for 1 min, and return to initial conditions and equilibrate for 0.5 min. Flow rate was 0.5 mL/min.

The mobile phase was delivered to an Agilent Jet Stream ESI source maintained in positive ion mode. MS/MS discrimination was performed via the multiple reaction monitoring (MRM) technique, incorporating isotope dilution. Two MRM transitions, quantification and confirmation, were monitored for each analyte. One MRM transition was monitored for each corresponding internal standard.

The monitored carfentanil-related transitions were *m/z* 395.2/335.4 (quantification; CE, 26 eV), *m/z* 395.2/246.2 (confirmation; CE, 31 eV), and *m/z* 400.2/340.4 (carfentanil-*d*<sub>5</sub> internal standard; CE, 26 eV). The monitored norcarfentanil-related transitions were *m/z* 291.0/231.0 (quantification; CE, 8 eV), *m/z* 291.0/175.0 (confirmation; CE, 12 eV), and *m/z* 296.0/236.0 (norcarfentanil-*d*<sub>5</sub> internal standard; CE, 8 eV). Capillary voltage, fragmenter voltage, and collision cell acceleration voltage were optimized to 1500, 380, and 5 V, respectively. Linear calibration curves (1/*x* weighting, analyte-to-ISTD peak area ratio) were generated for each analyte over the range of 1–1,000 µg/L.

For the RED experiments, the unbound fraction in plasma was calculated from the ratio of the average buffer side concentration to the average plasma side concentration. For the RBC/plasma partitioning experiments, the partition coefficient (log *P*) was calculated using the following equation (21):

$$K_{\frac{RBC}{PL}} = \frac{1}{H} \times \left( \frac{I_{PL}^{Ref}}{I_{PL}} - 1 \right) + 1 \quad (1)$$

where  $K_{\frac{RBC}{PL}}$  is the partition coefficient of the analyte in RBCs, *H* is the hematocrit,  $I_{PL}^{Ref}$  is the average analyte concentration in the reference plasma, and  $I_{PL}$  is the average analyte concentration in the test plasma.

## 2.4 In Vivo Exposure of Rabbits to Carfentanil

All animal exposures were conducted in accordance with guidance from the ECBC Institutional Animal Care and Use Committee (IACUC) under an approved animal use protocol. Four male NZWRs (Covance, Inc.; Denver, PA) were given 1 µg/kg iv bolus carfentanil doses (in sterile saline) in the marginal ear veins. At study initiation, the rabbits weighed 2.49–2.63 kg. Blood samples were collected from the marginal ear veins of the other, non-injected ears, in tubes that contained lithium-ethylenediaminetetraacetic acid as the anticoagulant. Samples were collected pre-exposure and at 1, 5, 10, and 30 min, 1 h, and 24 h after the iv administration. Of the dosed animals, 100% collapsed and 75% were prostrate. All animals recovered to apparent normal behavior within 24 h. Plasma was collected and stored at –80 °C until analysis. Plasma carfentanil concentrations were determined by LC–MS/MS. Time zero (immediately after injection) values were calculated based on the 1 µg/kg dose, the

actual body weight of each rabbit, and a blood volume of 60 mL/kg (22). Two-phase decay analysis was performed using Prism v.7.02 software (GraphPad Software; La Jolla, CA).

## **2.5 Human and Rabbit PBPK Profile Simulations Using GastroPlus Software**

GastroPlus simulation software was used to predict the carfentanil PK profiles in humans and rabbits based on the species-specific physicochemical properties of the compound and the expected clearance. Specifically, the rabbit plasma protein binding was 83.3%, blood partitioning was 0.9287, and RLM-derived intrinsic clearance ( $CL_{int}$ ) values populated the rabbit PBPK simulation. All other parameters were set to the GastroPlus default settings. The PK profile, which was simulated with a 1  $\mu$ g/kg of body weight, iv-administered dose, was compared with those profiles obtained when following the same protocol for live rabbits. Based on in vivo findings, the rabbit PBPK model was associated with 100% collapse and prostration (both severe effects).

Human PBPK simulations were conducted similarly, by substituting human values for predicted values in a stepwise fashion: human plasma protein binding was 87.6%, blood partitioning was 0.2746, and  $CL_{int}$  was 16.2 mL/min/kg of weight and 89.35  $\mu$ L/min/mg of protein to assess extrapolation from HLMs to whole body clearance (23). The dose was optimized for the rabbit (1  $\mu$ g/kg) until it achieved the same peak plasma concentration and PK profile as the model-validated rabbit data. Applied human PBPK parameters included the default 70 kg, 30 year old male human physiology in the GastroPlus software.

## **3. RESULTS**

### **3.1 Carfentanil Stability Study in RLMs**

An RLM half-life of  $2.1 \pm 0.1$  min was calculated from log-linear transformation of carfentanil depletion over 1 h (Figure 2), translated to a microsomal  $CL_{int}$  of 336.1  $\mu$ L/min/mg of protein (24), and a predicted rabbit hepatic clearance of 19.8 mL/min/kg, based on a liver weight of 45.1 g/kg of body weight and a protein concentration of 109 mg of protein/g of liver weight for the NZWR (24–26). This clearance rate is 3.7 times faster than the clearance for HLMs (7.8 min).



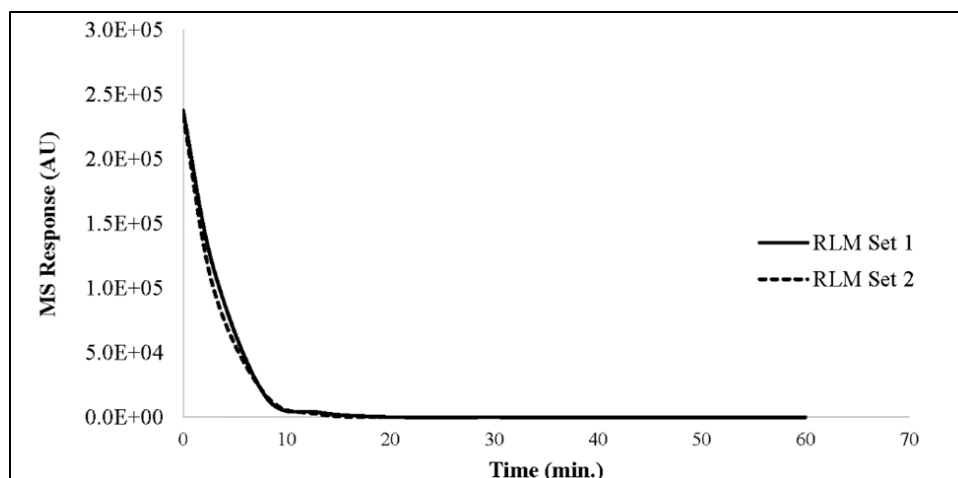


Figure 2. Parent compound depletion of carfentanil in RLM incubation. Study was performed in duplicate. Half-life was calculated to be 2.1 min.

### 3.2 Physicochemical Properties for HLMs and Hepatocytes

Although potency is an important aspect of a drug's pharmacological action, its absorption, distribution, metabolism, and excretion (ADME) paradigm is also important. The log  $P$ , plasma protein binding, and blood partitioning values contribute to ADME and were previously unknown for carfentanil and norcarfentanil. We determined these values to explain metabolism differences that were observed when HLMs and human hepatocytes were incubated with carfentanil (12). The physicochemical properties for both were time- and concentration-dependent; 30 min for protein binding and 60 min for blood/plasma partitioning are reported (Table 2; top and middle panes).

### 3.3 In Silico Predictions of Physicochemical Properties

The in silico predictions of physicochemical properties that were obtained using the Simulations Plus ADMET Predictor were based on the two-dimensional structures of carfentanil and norcarfentanil. The predicted properties did not correspond well with the experimentally derived values (Table 2, bottom). Plasma protein binding was over-predicted in both cases, and blood/plasma partitioning coefficients were under-predicted.

Table 2. Physicochemical Properties of Carfentanil with Benchmark Compound Fentanyl and Carfentanil Metabolite Norcarfentanil\*

Conc. (μM)	Human Protein Binding (Total %)			Rabbit Protein Binding (Total %)		
	Fentanyl	Carfentanil	Norcarfentanil	Fentanyl	Carfentanil	Norcarfentanil
1	88.3	87.6	11.3	80.9	83.3	27.8
10	86.7	83.8	10.9	75.4*	82.8	30.7

Conc. (nM)	Human Blood Partitioning			Rabbit Blood Partitioning		
	Fentanyl	Carfentanil	Norcarfentanil	Fentanyl	Carfentanil	Norcarfentanil
30	1.0656	0.2746	1.2063	0.8643	0.9287	1.5594
500	0.8295	0.7685	0.8499	1.3041	0.9681	1.1860

Predicted Property	Carfentanil	Norcarfentanil
log <i>P</i>	3.8	1.3
Protein binding	92.7	42.8
Blood/plasma partitioning	0.7	0.8

\*Plasma protein binding conducted by depletion (top pane) and blood partitioning (middle pane) were performed in rabbit and human tissues for use in the species-appropriate simulated physiology in the PBPK model. In silico predicted values from Simulations Plus ADMET Predictor are shown for general information for octanol–water partitioning coefficient (log *P*) and for comparison with experimental plasma protein binding, expressed as percent bound, and blood partitioning ratio.

### 3.4 In Vivo PK Study of Carfentanil in Rabbits

A single-bolus carfentanil dose of 1.0 μg/kg of body weight in four male NZWRs yielded a PK curve that indicated rapid redistribution from the central compartment and slower clearance from the blood had occurred. The two-phase decay half-life of carfentanil was calculated to be  $2.6 \times 10^{-8}$  min for the redistribution phase and 6.09 min for the clearance phase (regression coefficient [ $R^2$ ] of 0.9995) (Figure 3).

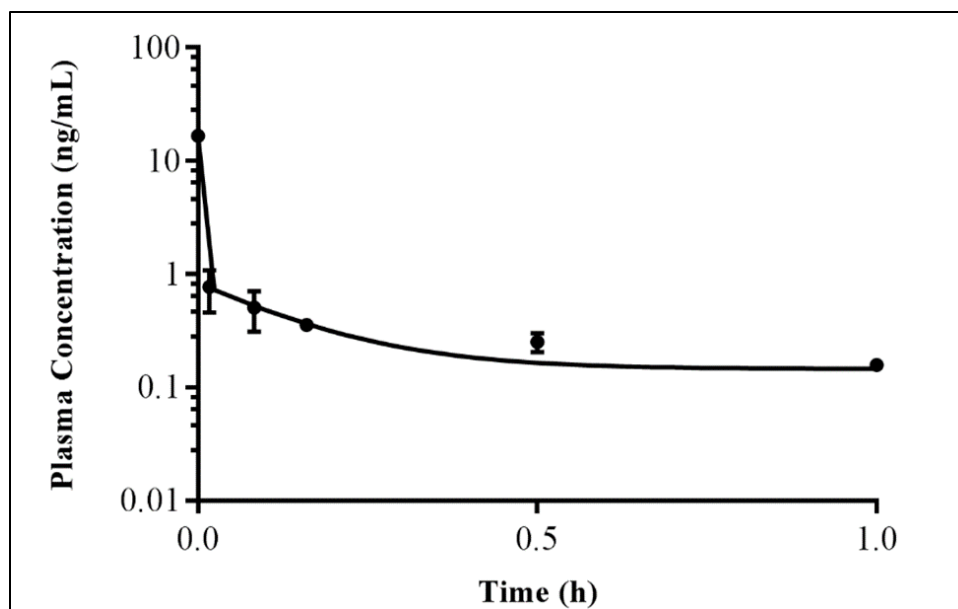


Figure 3. PK data for NZWRs dosed at 1  $\mu\text{g}/\text{kg}$  of carfentanil. Plotted as mean plasma concentrations with error bars as standard deviations (SDs;  $n = 4$ ).

### 3.5 In Silico Modeling of Rabbit PK

Modeling the actual PK data in a naïve model was slightly under-predictive of overall carfentanil clearance (Figure 4). The predicted plasma concentrations (solid line) were higher than those observed (black dots). As stated previously, metabolism (i.e., clearance) is the most influential parameter in most PBPK models (11), and it was obviously under-predicted in this naïve model. Additionally, it can be observed that the initial redistribution phase is not nearly rapid enough in the predicted model. This is not due to clearance, but is a result of the physicochemical properties, likely the blood partitioning. Redistribution influenced by blood partitioning is the most impactful property that can act rapidly to affect the first few minutes of the model. With no experimental data, the predicted PK is parallel to the actual PK but slightly higher. If nothing was known about this compound, this prediction would not be an unreasonable place to start (considering it overestimates the plasma levels, and subsequently, the toxicity). It would be a prudent and conservative place to begin with an unknown toxicant.

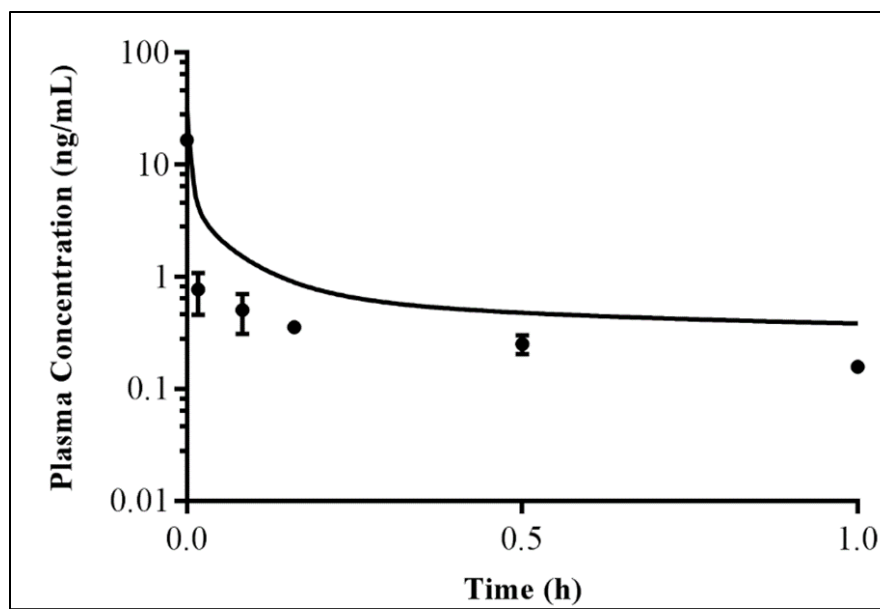


Figure 4. Naïve PBPK model obtained using only predicted ADMET Predictor properties, based on the two-dimensional structure of carfentanil. Line represents predicted PK. Dots represent actual in vivo data. Error bars are SDs of actual plasma concentrations.

Because metabolism is the most influential parameter to change in a PBPK model, this was added first (Figure 5). Compared with the purely in silico predicted model, incorporation of the experimentally derived  $CL_{int}$  yields data that are closer to the observed in vivo PK values for the later time points only. This appears to agree with results for analogous compounds that are better studied. Fentanyl was shown to undergo a three-phase PK curve: rapid redistribution, slower distribution, and finally, an elimination phase (27). The first two phases would likely not be highly influenced by clearance, but by physicochemical properties that dictate their redistribution.

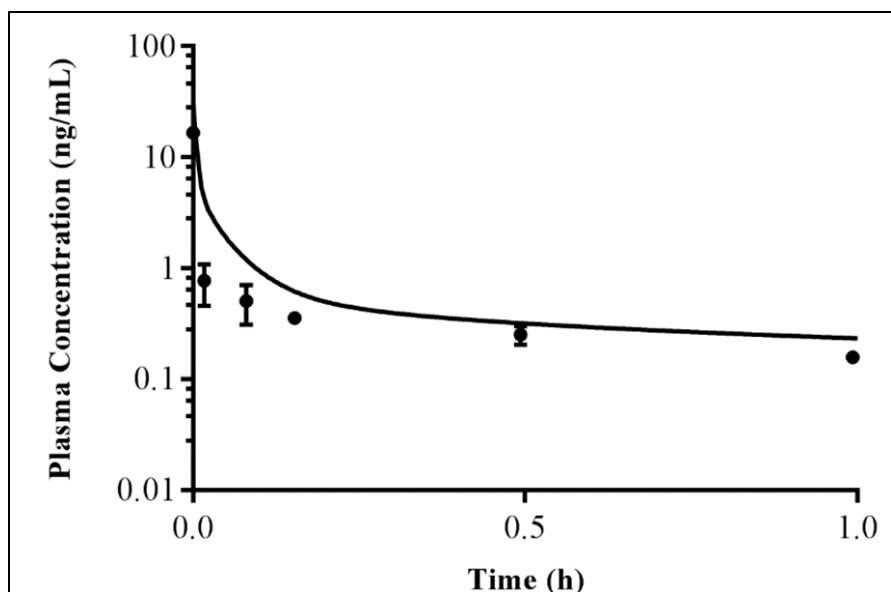


Figure 5. PBPK model incorporating only  $CL_{int}$ . Experimental data. Line represents predicted PK. Dots represent actual in vivo data. Error bars are SDs of actual plasma concentrations.

Following a stepwise approach, the plasma protein binding property was added to the model, without clearance, to see what effect it had on the PK prediction alone (Figure 6). This property had the least influence.

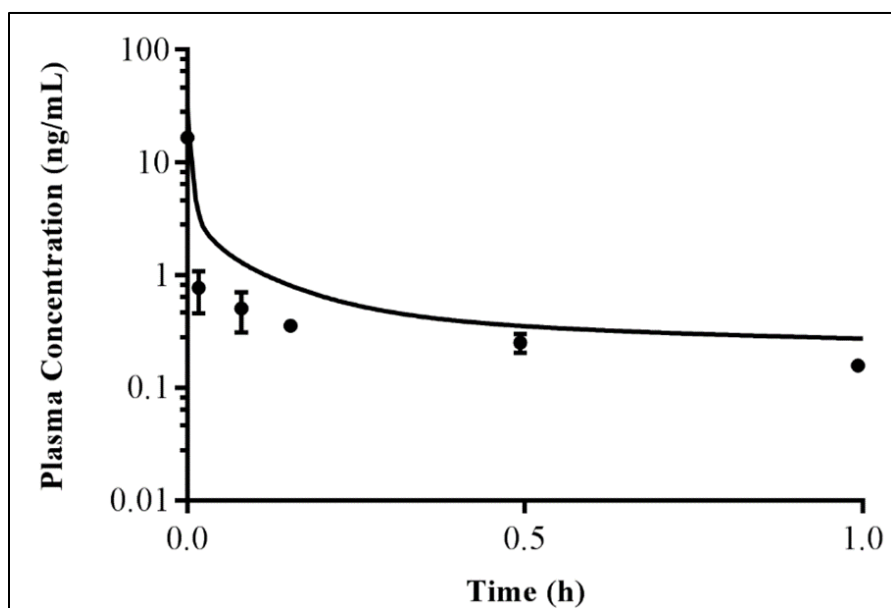


Figure 6. PBPK prediction incorporating only plasma protein binding experimental data. Line represents predicted PK. Dots represent actual in vivo data. Error bars are SDs of actual plasma concentrations.

The next PBPK model evaluated how the experimentally derived blood partitioning value improved the model (Figure 7). This property accounts for the “shoulder” in the PBPK curve that is shown in the in vivo PK profile. Blood partitioning plays a larger role than anticipated in influencing rapid (phase I) and slower (phase II) distribution from the central compartment. However, without clearance and plasma protein binding contributing to the third elimination phase, the later time points are still over-predicted.

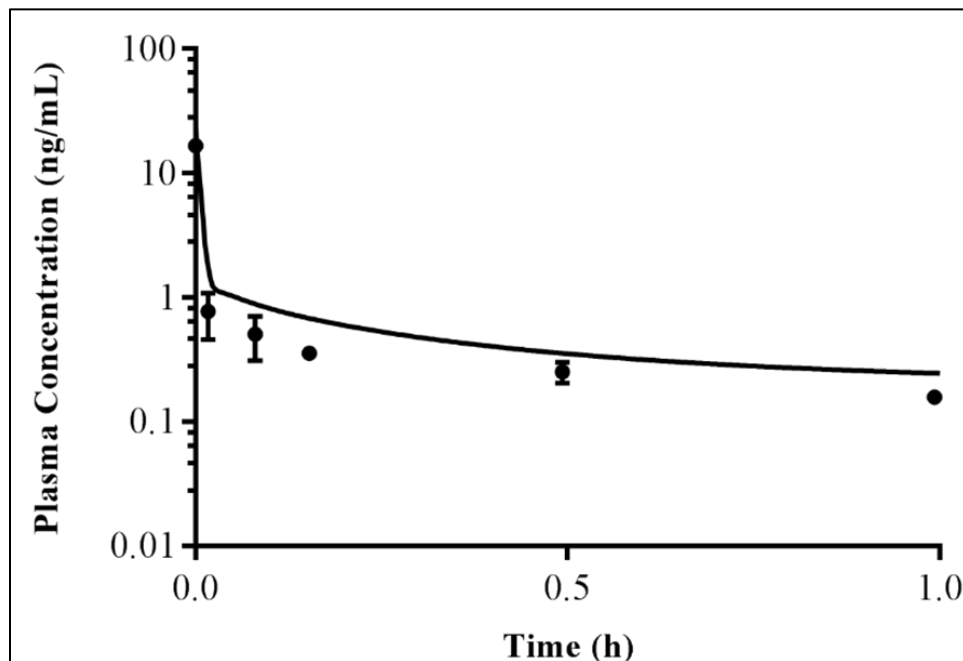


Figure 7. PBPK model incorporating only RBC plasma partitioning (RBP). Experimental data. Line shows predicted PK. Dots represent actual in vivo data. Error bars are SDs of actual plasma concentrations.

Finally, all three in vitro properties were incorporated into a single model (Figure 8). It is apparent that blood partitioning, as shown previously, affects the distribution phase, increasing the apparent clearance within the first few minutes. This is more representative of observed values in vivo. Plasma protein binding and  $CL_{int}$  have more effect on the phase II distribution and elimination. Although the PBPK model does not directly predict experimental values, it closely approximates the overall PK profile.

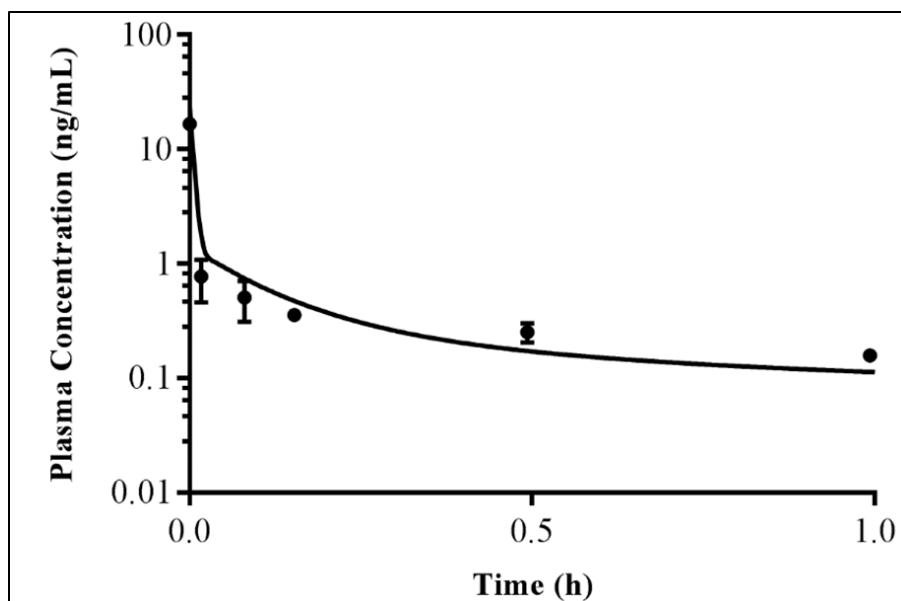


Figure 8. PBPK model incorporating  $CL_{int}$ , RBP, and plasma protein binding. Experimental data. Line shows predicted PK. Dots represent actual in vivo data. Error bars are SDs of actual plasma concentrations.

### 3.6 In Silico Prediction of Bioequivalent Dose of Carfentanil

The predictive power of the carfentanil–rabbit PBPK model can be improved simply by adding a few key properties into the simulation, namely,  $CL_{int}$ , plasma protein binding, and blood partitioning. This model transitioned from being under-predictive for carfentanil PK by iv administration in the rabbit in its naïve state, to more representative of in vivo PK, by populating the model with experimental data. The final step in this model-building exercise was to attempt to equate this to a human-equivalent dose using plasma concentration as the metric of bioequivalence (Figure 9).

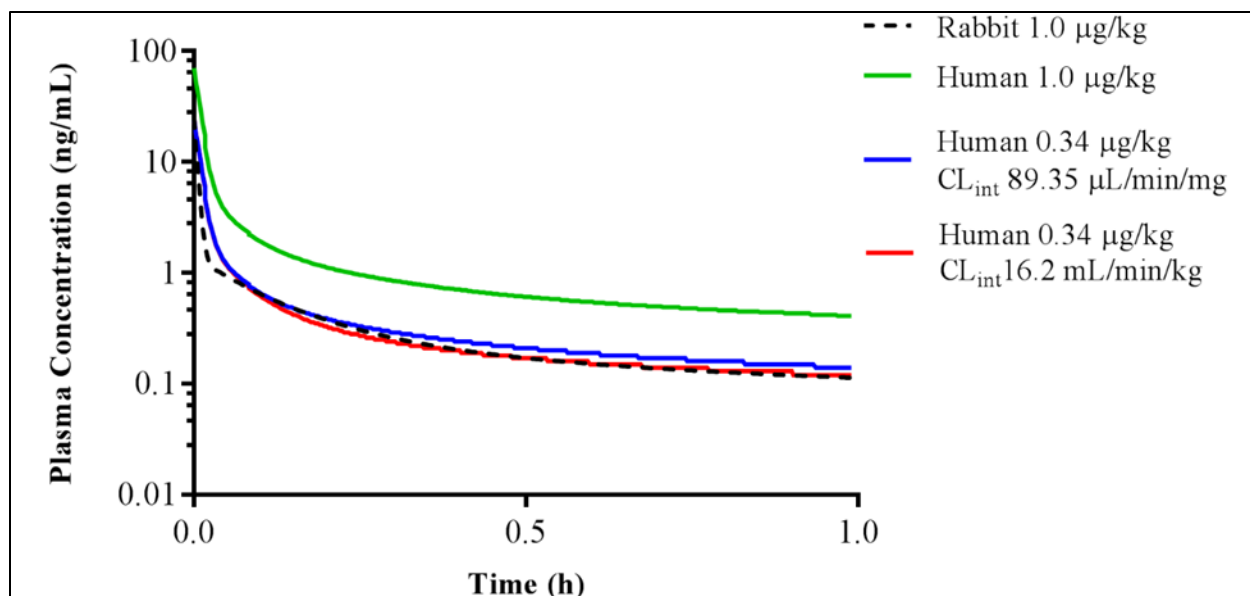


Figure 9. Human-equivalent dosing of carfentanil extrapolated from in silico model of rabbit PK data.

The direct equivalent dose (by mass) to the human achieves roughly three times the maximum plasma concentration. When the dose is lowered by  $\sim 1/3$ , the predicted plasma concentrations align closely between predicted plots for humans and rabbits. The prediction lies nearly on top of the rabbit PK prediction upon changing the unit of intrinsic clearance from that directly measured by HLM clearance ( $89.35 \mu\text{L}/\text{min}/\text{mg}$  protein) to the extrapolated organ clearance ( $16.2 \text{ mL}/\text{min}/\text{kg}$  body weight) (23), thereby demonstrating higher accuracy.

#### 4. DISCUSSION AND CONCLUSIONS

We present, for the first time, a novel way of generating an estimate of human toxicity from a unique combination of in vitro, in silico, and a small number of in vivo experiments. This study provides important new data on the physicochemical properties of carfentanil and norcarfentanil in rabbit and human blood. Available experimental data for carfentanil are vital to the PK modeling. Plasma protein binding and blood partitioning contribute strongly to in vivo PK and the in silico modeling of kinetics. This is because they have a large role in determining the absorptive, distributive, and metabolic properties. These properties impact how much carfentanil is in various tissue compartments (and the volume of distribution); and how much is in the systemic circulation and available to cross the blood–brain barrier, act on its target receptors, or be cleared by metabolizing organs and enzymes. Together, all of these properties determine overall exposure intensity, duration, and subsequently, toxicity. These data also provide useful tools for performing forensic or analytical chemical analysis on carfentanil-containing samples. This information, combined with the microsomal stability and metabolism study, yields a better understanding of carfentanil PK.



We demonstrated that accurate predictions can be achieved by populating the in silico model with experimental data. Furthermore, by using in vitro data from multiple species, human extrapolation can achieve realistic predictive power. Specifically, this was achieved by measuring carfentanil clearance in RLMs, plasma protein binding in rabbit plasma, and blood partitioning in rabbit whole blood, and then populating the in silico rabbit physiology with these values. Upon switching to the human physiology for translation, HLM clearance data, human plasma protein binding, and human blood partitioning were used to populate the human physiology for dose equivalence.

In silico PBPK modeling is valuable when translating from an animal model and/or in vitro data to a human model. There are limited human carfentanil administration data and subsequent PK properties. In all studies where humans were given carfentanil, it was for the purpose of mapping mu opioid receptors in the brain using positron emission tomography scanning, or in one case, measuring the dosimetry of the carfentanil radioisotope (28–31).

When translating from a surrogate animal model to human PBPK simulation with GastroPlus software, the most important factor was clearance rate.  $CL_{int}$  was calculated to be 3.7× faster in RLMs than HLMs. The human-equivalent dose was roughly one-third of that for rabbits, and this is likely attributable to humans having one-third the metabolic clearance potential. The remainder of that difference is likely due to the slight differences in the physicochemical properties from the in silico predicted values. Together, the in silico model provided accurate PBPK of carfentanil exposure when used in conjunction with key experimentally derived property values (in this case, plasma protein binding and blood partitioning).

In addition to the better fit of the PBPK model to the in vivo data and the human-equivalence dosing to achieve similar PBPK, the keystone of this research is perhaps the plausibility of the human predicted dose for carfentanil toxicity (Table 3). The model provides an estimate for a human dose that achieved a “severely toxic” endpoint in the rabbit surrogate (0.34 µg/kg), namely, collapse and prostrate. Previous studies in humans showed successful administration of <sup>11</sup>C-carfentanil at doses of 0.03 µg/kg with only reports of drowsiness in some patients (31).

The administered human dose reported is almost exactly one order of magnitude less than the predicted toxic dose. Therefore, this predicted human toxic dose agrees with the therapeutic index of 10 reported for carfentanil in nonhuman primates (32).

Table 3. Therapeutic Toxic Doses for Carfentanil in Monkeys (Port et al.) and Humans (Newberg et al.) and Their Respective Therapeutic Indices\*

	<b>Effective Dose (µg/kg)</b>	<b>Toxic Dose (µg/kg)</b>	<b>Therapeutic Index</b>
Nonhuman primate	0.1	1	10
Human	0.03	0.34 (predicted)	11

\*Carfentanil toxic dose generated in this study.

To further corroborate the plausibility of this human risk assessment for carfentanil is the reported lethal dose by the DEA. Their predicted lethal dose of carfentanil in humans is 0.29  $\mu\text{g}/\text{kg}$ , or 20  $\mu\text{g}$  for a 70 kg human (6). This differs by the human risk assessment present here by only 50  $\text{ng}/\text{kg}$ , which is an arguably negligible amount. Although this study relied on *in silico* and *in vitro* methods for risk assessment, the rationale for the predicted value presented by the DEA is unclear, but it does not appear to be based on human or other animal physiology.

As demonstrated here, by using *in silico* and *in vitro* technologies, *in vivo* experimentation can be refined, reduced, and potentially replaced as we work effectively and efficiently toward physiologically based human-relevant toxicity estimates.

## LITERATURE CITED

1. Kounang, N. Elephant Tranquilizer to Blame for At Least 8 Ohio Deaths. CNN Health, 7 September 2016. <https://www.cnn.com/2016/09/06/health/carfentanil-deaths-ohio/index.html> (accessed 12 July 2018).
2. Kounang, N.; Marco, T. Heroin Laced with Elephant Tranquilizer Hits the Streets. CNN Health, 25 August 2016. <https://www.cnn.com/2016/08/24/health/elephant-tranquilizer-carfentanil-heroin/index.html> (accessed 12 July 2018).
3. Medical Examiner Public Health Warning: Deadly Carfentanil Has Been Detected in Cuyahoga County. Cuyahoga County, Ohio Office of the Executive, 18 August 2016. <http://executive.cuyahogacounty.us/en-us/me-public-health-warning.aspx> (accessed 12 July 2018).
4. Riches, J.R.; Read, R.W.; Black, R.M.; Cooper, N.J.; Timperley, C.M. Analysis of Clothing and Urine from Moscow Theatre Siege Casualties Reveals Carfentanil and Remifentanil Use. *J. Anal. Toxicol.* **2012**, *36*, 647–656.
5. Wax, P.M.; Becker, C.E.; Curry, S.C. Unexpected “Gas” Casualties in Moscow: A Medical Toxicology Perspective. *Ann. Emerg. Med.* **2003**, *41*, 700–705.
6. Casale, J.F.; Mallette, J.R.; Guest, E.M. Analysis of Illicit Carfentanil: Emergence of the Death Dragon. *Forensic Chem.* **2017**, *3*, 74–80.
7. Feldman, P.L.; James, M.K.; Brackeen, M.F.; Bilotta, J.M.; Schuster, S.V.; Lahey, A.P.; Lutz, M.W.; Johnson, M.R.; Leighton, H.J. Design, Synthesis, and Pharmacological Evaluation of Ultrashort- to Long-Acting Opioid Analgetics. *J. Med. Chem.* **1991**, *34*, 2202–2208.
8. Flecknell, P.A.; Liles, J.H.; Wootton, R. Reversal of Fentanyl/Fluanisone Neuroleptanalgesia in the Rabbit Using Mixed Agonist/Antagonist Opioids. *Lab. Anim.* **1989**, *23*, 147–155.
9. Hyatt, J.; Coro, C.; Bergman, S.A.; Wynn, R.L. Effects of Midazolam on Fentanyl Antinociception and Respiration in a Rabbit Model. *J. Oral Maxillofac. Surg.* **1989**, *47*, 1298–1302.
10. Stephen, G.W.; Cooper, L.V. The Role of Analgesics in Respiratory Depression: A Rabbit Model. *Anaesthesia* **1977**, *32*, 324–327.
11. Espi e, P.; Tytgat, D.; Sargentini-Maier, M.L.; Poggesi, I.; Watelet, J.B. Physiologically Based Pharmacokinetics (PBPK). *Drug Metab. Rev.* **2009**, *41*, 391–407.
12. Feasel, M.G.; Wohlfarth, A.; Nilles, J.M.; Pang, S.; Kristovich, R.L.; Huestis, M.A. Metabolism of Carfentanil, An Ultra-Potent Opioid, in Human Liver Microsomes and Human Hepatocytes by High-Resolution Mass Spectrometry. *AAPS J.* **2016**, *18*, 1489–1499.
13. Deshmukh, P.V.; Badgajar, P.C.; Gatne, M.M. In-Vitro Red Blood Cell Partitioning of Doxycycline. *Indian J. Pharmacol.* **2005**, *41*, 173–175.

14. Tetko, I.V.; Gasteiger, J.; Todeschini, R.; Mauri, A.; Livingstone, D.; Ertl, P.; Palyulin, V.A.; Radchenko, E.V.; Zefirov, N.S.; Makarenko, A.S.; Tanchuk, V.Y.; Prokopenko, V.V. Virtual Computational Chemistry Laboratory—Design and Description. *J. Comput. Aided Mol. Des.* **2005**, *19*, 453–463.
15. Virtual Computational Chemistry Laboratory, 2005–2016. [www.vcclab.org](http://www.vcclab.org) (accessed 16 July 2018).
16. Hinderling, P.H. Red Blood Cells: A Neglected Compartment in Pharmacokinetics and Pharmacodynamics. *Pharmacol. Rev.* **1997**, *49*, 279–295.
17. Bista, S.R.; Haywood, A.; Hardy, J.; Lobb, M.; Tapuni, A.; Norris, R. Protein Binding of Fentanyl and Its Metabolite Nor-Fentanyl in Human Plasma, Albumin and  $\alpha$ -1 Acid Glycoprotein. *Xenobiotica* **2015**, *45*, 207–212.
18. Ishizaki, J.; Yokogawa, K.; Nakashima, E.; Ichimura, F. Relationships between the Hepatic Intrinsic Clearance or Blood Cell-Plasma Partition Coefficient in the Rabbit and the Lipophilicity of Basic Drugs. *J. Pharm. Pharmacol.* **1997**, *49*, 768–772.
19. Campbell, J.L., Jr.; Clewell, R.A.; Gentry, P.R.; Andersen, M.E.; Clewell, H.J., III. Physiologically Based Pharmacokinetic/Toxicokinetic Modeling. *Method. Mol. Biol.* **2012**, *929*, 439–499.
20. Wang, L.; Bernert, J.T. Analysis of 13 Fentanils, including Sufentanil and Carfentanil, in Human Urine by Liquid Chromatography–Atmospheric-Pressure Ionization–Tandem Mass Spectrometry. *J. Anal. Toxicol.* **2006**, *30*, 335–341.
21. Yu, S.; Li, S.; Yang, H.; Lee, F.; Wu, J.-T.; Qian, M.G. A Novel Liquid Chromatography/Tandem Mass Spectrometry-Based Depletion Method for Measuring Red Blood Cell Partitioning of Pharmaceutical Compounds in Drug Discovery. *Rapid Commun. Mass Spectrom.* **2005**, *19*, 250–254.
22. Suckow, M.A.; Schroeder, V.; Douglas, F.A. *The Laboratory Rabbit*, 2nd ed.; CRC Press: Boca Raton, FL, 2010.
23. McNaney, C.A.; Drexler, D.M.; Hnatyshyn, S.Y.; Zvyaga, T.A.; Knipe, J.O.; Belcastro, J.V.; Sanders, M. An Automated Liquid Chromatography–Mass Spectrometry Process to Determine Metabolic Stability Half-Life and Intrinsic Clearance of Drug Candidates by Substrate Depletion. *Assay Drug Dev. Technol.* **2008**, *6*, 121–129.
24. Lavé, T.; Dupin, S.; Schmitt, C.; Valles, B.; Ubead, G.; Chou, R.C.; Jaeck, D.; Coassolo, P. The Use of Human Hepatocytes to Select Compounds Based on Their Expected Hepatic Extraction Ratios in Humans. *Pharm. Res.* **1997**, *14*, 152–155.
25. Jelenko, C., III; Anderson, A.P.; Scott, T.H., Jr.; Wheeler, M.L. Organ Weights and Water Composition of the New Zealand Albino Rabbit (*Oryctolagus cuniculus*). *Am. J. Vet. Res.* **1971**, *32*, 1637–1639.
26. Sohlenius-Sternbeck, A.K. Determination of the Hepatocellularity Number for Human, Dog, Rabbit, Rat and Mouse Livers from Protein Concentration Measurements. *Toxicol. In Vitro* **2006**, *20*, 1582–1586.
27. Halliburton, J.R. The Pharmacokinetics of Fentanyl, Sufentanil and Alfentanil: A Comparative Review. *AANA J.* **1988**, *56*, 229–233.

28. Endres, C.J.; Bencherif, B.; Hilton, J.; Madar, I.; Frost, J.J. Quantification of Brain  $\mu$ -Opioid Receptors with [ $^{11}\text{C}$ ]Carfentanil: Reference-Tissue Methods. *Nucl. Med. Biol.* **2003**, *30*, 177–186.
29. Newman, A.; Channing, M.; Finn, R.; Dunn, B.; Simpson, N.; Carson, R.; Ostrowski, N.; Cohen, R.; Burke, T.; Larson, S.; Rice, K. Ligands for Imaging Opioid Receptors in Conscious Humans by Positron Emission Tomography (PET). *NIDA Res. Monog.* **1988**, *90*, 117–121.
30. Villemagne, P.S.; Dannals, R.F.; Ravert, H.T.; Frost, J.J. PET Imaging of Human Cardiac Opioid Receptors. *Eur. J. Nucl. Med. Mol. Imaging* **2002**, *29*, 1385–1388.
31. Newberg, A.B.; Ray, R.; Scheuermann, J.; Wintering, N.; Saffer, J.; Freifelder, R.; Karp, J.; Lerman, C.; Divgi, C. Dosimetry of  $^{11}\text{C}$ -Carfentanil, a  $\mu$ -Opioid Receptor Imaging Agent. *Nucl. Med. Commun.* **2009**, *30*, 314–318.
32. Port, J.D.; Stanley, T.H.; Steffey, E.P.; Pace, N.L.; Henrickson, R.; McJames, S.W. Intravenous Carfentanil in the Dog and Rhesus Monkey. *Anesthesiology* **1984**, *61*, A378.

Blank

## ACRONYMS AND ABBREVIATIONS

ACN	acetonitrile
ADME	absorption, distribution, metabolism, and excretion
BEH	ethylene-bridged hybrid
CE	collision energy
CL <sub>int</sub>	intrinsic clearance
CXP	collision cell exit potential
DEA	U.S. Drug Enforcement Administration
dH <sub>2</sub> O	deionized water
DMSO	dimethyl sulfoxide
DP	declustering potential
EP	entrance potential
ESI	electrospray ionization
ECBC	U.S. Army Edgewood Chemical Biological Center
HLM	human liver microsome
IACUC	Institutional Animal Care and Use Committee
ISTD	isotopically labeled internal standard
iv	intravenous
LC	liquid chromatography
MRM	multiple reaction monitoring
MS	mass spectrometry
<i>m/z</i>	charge-to-mass ratio
NADPH	reduced nicotinamide adenine dinucleotide phosphate
NMR	nuclear magnetic resonance
NZWR	New Zealand White rabbit
PBPK	physiologically based pharmacokinetic
PBS	phosphate-buffered saline
PK	pharmacokinetics
<i>R</i> <sup>2</sup>	regression coefficient
RBC	red blood cell
RBP	red blood cell plasma partitioning
RED	rapid equilibrium dialysis
RLM	rabbit liver microsome
SD	standard deviation





## DISTRIBUTION LIST

The following individuals and organizations were provided with one Adobe portable document format (pdf) electronic version of this report:

U.S. Army Edgewood Chemical  
Biological Center (ECBC)  
Operational Toxicology Branch  
RDCB-DRT-O  
ATTN: Feasel, M.  
Whalley, C.

Defense Threat Reduction Agency  
J9-CBS  
ATTN: Director-Myska, A.  
Peacock-Clark, S.  
Minyard, M.  
Cronce, D.  
Vann, B.

Defense Technical Information Center  
ATTN: DTIC OA

G-3 History Office  
U.S. Army RDECOM  
ATTN: Smart, J.

ECBC Technical Library  
RDCB-DRB-BL  
ATTN: Foppiano, S.  
Stein, J.

Office of the Chief Counsel  
AMSRD-CC  
ATTN: Upchurch, V.

